PHILOSOPHICAL TRANSACTIONS OF THE ROYAL SOCIETY A MATHEMATICAL, PHYSICAL & ENGINEERING SCIENCES

# A Comparison of One-, Two- and Three-Dimensional Model Representations of Stratospheric Gases [and Discussion]

A. F. Tuck, R. A. Scriven and D. T. Swift-Hook

*Phil. Trans. R. Soc. Lond. A* 1979 **290**, 477-494
doi: 10.1098/rsta.1979.0008

*Phil. Trans. R. Soc. Lond.* A. **290**, 477–494 (1979)
*Printed in Great Britain*



# A comparison of one-, two- and three-dimensional model representations of stratospheric gases

By A. F. Tuck
*Meteorological Office, London Road, Bracknell, RG12 2SZ, U.K.*

Three- and two-dimensional model results have been averaged to investigate conceptual errors in two- and one-dimensional models. Average dynamical quantities show inter-hemispheric asymmetries in both mean and eddy vertical motions, with anomalous behaviour of tracers near effective source and sink regions.

Zonal, hemispheric and global means of the rates of gas reactions show large deviations between terms like $\overline{k[\mathrm{A}]\,[\mathrm{B}]}$ and $\bar{k}\overline{[\mathrm{A}]\,[\mathrm{B}]}$, causing significant errors in two- and one-dimensional model calculations. These errors are often associated with dynamical features such as jet streams or the tropopause, and affect the entire model atmospheres except in the summer mid-stratosphere.

It is concluded that correlated measurements of atmospheric molecular number densities are urgently required to understand the deficiencies in models, which have been widely used to make perturbation calculations of the effects of aircraft and chlorofluoromethanes on stratospheric ozone. The sources of error described in this work arise from inadequacies in the formulation of one- and two-dimensional models, rather than from uncertainties in the input data, and have not been included in published error analyses.

## 1. Introduction

In order to calculate the chemical composition of the stratosphere, and possible perturbations to its distributions of molecules, it has been necessary to resort to numerical models in one, two and three dimensions.

A three-dimensional general circulation model (g.c.m.) of the atmosphere is based on the equations of motion for the wind components, the mass continuity equation, the equation of state and the thermodynamic equation. Integration of this set of equations with time yields values of the wind components, pressure, density and temperature on a grid of longitude, latitude and altitude. The rate of change of any gaseous constituent is given by an equation of the type

$$\partial\chi_{\mathrm{i}}/\partial t = P_{\mathrm{i}} - L_{\mathrm{i}} - \nabla . \boldsymbol{V}\chi_{\mathrm{i}}, \tag{1}$$

where $\chi_{\mathrm{i}}$ is mixing ratio, $P_{\mathrm{i}}$ is the local rate of production (source), $L_{\mathrm{i}}$ is the local rate of loss (sink) and the last term is the flux divergence caused by the wind velocity $\boldsymbol{V}$.

In a g.c.m. including the stratosphere it might be necessary to include up to 60 species for a complete representation of the photochemistry. In addition many physical processes such as radiative transfer, surface exchanges, subgrid scale convection, rainfall and the like must be included. This is not possible even with the largest and fastest machines presently available, and in practice no more than three or four species have been represented by an equation like (1).

Two-dimensional models economize on the number of grid points by averaging over longitude (i.e. round a latitude circle) and representing the variables as zonal means on a grid of latitude and altitude. One-dimensional models carry this process a stage further by averaging over latitude to represent the atmospheric variables in a single vertical column.

It will be seen in § 2 that this averaging process raises questions about how accurately models of reduced dimensionality represent true zonal or global means of three-dimensional distributions of variables. The work described here seeks to investigate this question by using results from Meteorological Office models. Mahlman (1976) has also considered these problems.

There is beyond this, of course, the more fundamental question of whether models of one, two or three dimensions mishandle correlations of variables occurring in the real atmosphere on scales not represented in the models. For example, it is likely that ascending air over the continents has a different chemical composition from that of descending air over the oceans. At any one time these air parcels cannot of course react chemically; however, such a distinction can only be made in a three-dimensional model, and then only on scales larger than its grid length. It thus follows that if it is desired, for example, to compute the mean global rate of a reaction

$$\mathrm{A}+\mathrm{B}\rightarrow\mathrm{C}+\mathrm{D}$$

characterized by rate coefficient $k$, it is in principle necessary to compute from observed number density distributions of A and B, pressure and temperature the local values of the rate $k[\mathrm{A}][\mathrm{B}]$, and obtain the global mean rate by averaging these local rates. This mean will be different from the mean computed by forming the product of the separate global means of $k$, [A] and [B], if any nonlinear correlations are present. The computation of zonal means in two-dimensional models and of global means in one-dimensional models is implicitly dependent upon the assumption that the true mean rate can be formed by the product of the means of $k$, [A] and [B].

The necessary observations of molecular number densities are not available, so the checking of the averaging process in one- and two-dimensional models unfortunately cannot be made with real data. However, it is possible for example to average data from a three-dimensional model to check both two- and one-dimensional calculations, and to average two-dimensional model results to check one-dimensional models. Questions as to the effect of averaging over different seasons and the two hemispheres may also be examined as part of this approach. The work described here has attempted to carry out such an investigation, and gives first results.

## 2. Equations and models

In three dimensions the behaviour of the mixing ratio $\chi$ of a constituent gas is given by

$$\frac{\partial\chi}{\partial t}+\frac{1}{r\cos\phi}\frac{\partial}{\partial\Lambda}u\chi+\frac{1}{r\cos\phi}\frac{\partial}{\partial\phi}v\chi\cos\phi+\frac{\partial}{\partial z}w\chi=P-L. \tag{2}$$

Here $P$ is source, $L$ is sink, $u$, $v$ and $w$ are respectively zonal, meridional and vertical velocities, $\phi$ is latitude, $\Lambda$ is longitude, $z$ is altitude and $t$ is time.

Reduction to two dimensions is achieved by the definition of the zonal mean of $\chi$ (denoted by an overbar)

$$\overline{\chi}=\frac{1}{2\pi}\int_0^{2\pi}\chi\,\mathrm{d}\Lambda. \tag{3}$$

This results in a relation which describes the time dependence of $\chi$ in the meridional and vertical directions:

$$\frac{\partial\overline{\chi}}{\partial t}+\frac{1}{r\cos\phi}\frac{\partial}{\partial\phi}\overline{v\chi}\cos\phi+\frac{\partial}{\partial z}\overline{w\chi}=\overline{P-L}. \tag{4}$$

An equation like (4) exists for each species and should in principle be integrated forward in time, with the dynamical terms on the left and the physico-chemical terms on the right evolving

simultaneously and interactively on the latitude–height grid. However, a full two-dimensional set of the equations of motion, thermodynamic equation and a continuity equation for each species demands in its solution a general theory connecting the eddy components with the mean components of $u$, $v$, $w$, $\chi$ and temperature $T$. This task has not in general been tackled by two-dimensional modellers. Instead an approach given originally by Reed & German (1965) has been widely adopted, in which climatological data are used for the mean meridional wind component $v$ in conjunction with a flux-gradient representation of the eddy terms derived from empirically obtained diffusivity coefficients.

The zonal mean $\bar{\chi}$ of equation (3) is used to define the local departures $\chi'$ from the average at any longitude:

$$\chi' = \chi - \bar{\chi}. \tag{5}$$

The zonal mean of $\chi'$ is zero, but products of primed quantities lead to the relations

$$\overline{v\chi} = \bar{v}\bar{\chi} + \overline{v'\chi'}; \tag{6}$$

$$\overline{w\chi} = \bar{w}\bar{\chi} + \overline{w'\chi'}. \tag{7}$$

The term on the left side of (6) and (7) is the mean total flux, and is equal to the sum of the flux $\bar{v}\bar{\chi}$ or $\bar{w}\bar{\chi}$ caused by the mean components and the eddy flux $\overline{v'\chi'}$ or $\overline{w'\chi'}$ arising from correlations between local departures from zonal averages at different longitudes.

The Reed & German (1965) approach results in expressions of the form

$$\overline{v'\chi'} = -\left(K_{yy}\frac{\partial\bar{\chi}}{\partial y} + K_{yz}\frac{\partial\bar{\chi}}{\partial z}\right); \tag{8}$$

$$\overline{w'\chi'} = -\left(K_{zy}\frac{\partial\bar{\chi}}{\partial y} + K_{zz}\frac{\partial\bar{\chi}}{\partial z}\right). \tag{9}$$

The theory requires $K_{yy}$ and $K_{zz}$ to be positive, but $K_{yz}$ ($\approx K_{zy}$) may be of either sign. Methods of obtaining these coefficients have been discussed in various places (Reed & German 1965; Gudiksen *et al.* 1968; Luther 1973). The further averaging of the two-dimensional model over latitude to produce a one-dimensional model immediately produces a dilemma as to whether the resulting column should be chosen to represent global or hemispheric behaviour. The derivation of global and hemispheric models will be given in parallel.

To obtain one-dimensional equations from equation (4), it is necessary to define global/hemispheric averages by the following relations. Globally,

$$\langle\chi\rangle = \frac{1}{2}\int_{-\frac{1}{2}\pi}^{\frac{1}{2}\pi}\bar{\chi}\cos\phi\,\mathrm{d}\phi; \tag{10a}$$

hemispherically,

$$\langle\langle\chi\rangle\rangle = \int_{0}^{\frac{1}{2}\pi}\bar{\chi}\cos\phi\,\mathrm{d}\phi. \tag{10b}$$

Here, the single angle brackets denote a global mean and the double angle brackets a hemispheric mean. These lead respectively to one-dimensional equations

$$\frac{\partial\langle\chi\rangle}{\partial t} + \frac{\partial}{\partial z}\langle w\chi\rangle = \langle P - L\rangle, \tag{11a}$$

$$\frac{\partial\langle\langle\chi\rangle\rangle}{\partial t} + \frac{(\overline{v\chi})_{\text{equator}}}{r} + \frac{\partial}{\partial z}\langle\langle w\chi\rangle\rangle = \langle\langle P - L\rangle\rangle. \tag{11b}$$

Equation 10*a* for air ($\chi = 1$) would lead to a latitude of 0° for the global average column, and (10*b*) would lead to 30° for the hemispheric average column. For species with $\chi$ much less than unity (i.e. all species except $N_2$ and $O_2$), the latitude should be at the centre of gravity of $c\cos\phi$ (Tuck 1977), with the difficulty that this may occur at different latitudes for different species. The global mean vertical velocity must be zero in the temporal mean, and hence (11*a*) is used in the form

$$\frac{\partial\langle\chi\rangle}{\partial t} = \frac{\partial\langle K_z\rangle}{\partial z}\frac{\partial\langle\chi\rangle}{\partial z} + \langle P - L\rangle, \tag{12}$$

where the global mean coefficient $\langle K_z\rangle$ is defined by

$$\langle w\chi\rangle = -\langle K_z\rangle\,\partial\langle\chi\rangle/\partial z \tag{13}$$

and represents total flux, making no distinction between mean and eddy motion. Equation (12) implies that total global mean vertical transport of a species is proportional to and down its gradient, and suffers further from the difficulty that air motions require the mean latitude to be 0°, while it is clear that if the insolation for the photochemistry is calculated at this latitude the resulting solar fluxes will not represent a global average. Any effects such as seasonal differences or hemispheric asymmetries are averaged out.

A hemispheric equation analogous to (12) may be obtained from (11*b*):

$$\frac{\partial\langle\langle\chi\rangle\rangle}{\partial t} = \frac{\partial}{\partial z}\langle\langle K_z\rangle\rangle\frac{\partial\langle\langle\chi\rangle\rangle}{\partial z} - \frac{(\overline{v\chi})_{\text{equator}}}{r} - \frac{\partial}{\partial z}(\langle\langle w\rangle\rangle\langle\langle\chi\rangle\rangle) + \langle\langle P - L\rangle\rangle, \tag{14}$$

where the hemispheric vertical flux is resolved into mean and eddy components:

$$\langle\langle w\chi\rangle\rangle = -\langle\langle K_z\rangle\rangle\,\partial\langle\langle\chi\rangle\rangle/\partial z + \langle\langle w\rangle\rangle\langle\langle\chi\rangle\rangle. \tag{15}$$

If it is desired to investigate such effects as seasonal variations, hemispherical differences and the relative importance of mean and eddy motions in the vertical, a one-dimensional model must be based on (14) rather than (12). In general, hemispheric mean vertical velocities would be extremely difficult to compute from real data; here, three-dimensional model data have been used.

The practical formulation of a one-dimensional model from (14) involves rewriting the two-dimensional equation (4) in terms of number densities:

$$\frac{\partial\bar{n}}{\partial t} + \frac{1}{r}\frac{\partial(\overline{nv})}{\partial\phi} - \overline{nv}\frac{\tan\phi}{r} + \frac{\partial(\overline{nw})}{\partial z} = \overline{P^\dagger - L^\dagger}, \tag{16}$$

where $P^\dagger$ and $L^\dagger$ now refer to number densities rather than mixing ratios.

By writing $y = r\phi$, and assuming that mass continuity relates $\bar{v}$ and $\bar{w}$ it may be shown that to a good approximation

$$\frac{\partial\bar{v}}{\partial y} - \bar{v}\frac{\tan\phi}{r} + \frac{\partial\bar{w}}{\partial z} = 0. \tag{17}$$

This relation makes it clear that a one-dimensional model representing a hemisphere must have a column in the opposite hemisphere from which to supply horizontal flow to satisfy mass continuity when the hemispheric mean vertical velocity is non-zero. It is thus in a sense two-dimensional; it may be made effectively one-dimensional by treating one of the columns as a boundary, with prescribed values.

From (16),

$$\frac{\partial\bar{n}}{\partial t} + \frac{\partial(\overline{nv})}{\partial y} - \overline{nv}\frac{\tan\phi}{r} + \frac{\partial(\overline{nw})}{\partial z} = \overline{P^\dagger - L^\dagger}. \tag{18}$$

By using (6) to (9) in number density form, differentiating products and noting (17),

$$\frac{\partial \bar{n}}{\partial t}+\bar{w}\frac{\partial \bar{n}}{\partial z}-\frac{\partial}{\partial z}\rho\left\{K_{zy}\frac{\partial}{\partial y}\frac{\bar{n}}{\rho}+K_{zz}\frac{\partial}{\partial z}\frac{\bar{n}}{\rho}\right\}+\bar{v}\frac{\partial \bar{n}}{\partial y}-\frac{\partial}{\partial y}\rho\left\{K_{yy}\frac{\partial}{\partial y}\frac{\bar{n}}{\rho}+K_{yz}\frac{\partial}{\partial z}\frac{\bar{n}}{\rho}\right\}$$
$$+\rho\left\{K_{yy}\frac{\partial}{\partial y}\frac{\bar{n}}{\rho}+K_{yz}\frac{\partial}{\partial z}\frac{\bar{n}}{\rho}\right\}\frac{\tan\phi}{r}=\overline{P^{\dagger}-L^{\dagger}}, \qquad (19)$$

where $\rho$ is the air density.

The last four terms on the left side of (19) specify the mean and eddy components of the inter-hemispheric flow necessary to satisfy mass continuity. The remaining terms may be averaged by using (10*b*) to obtain the hemispheric one-dimensional form. In practice, hemispheric mean values, $\langle\langle w\rangle\rangle$, have been obtained from the Meteorological Office three-dimensional model (Comesa 1975; O'Neill & Newson 1977) on 13 levels up to 44 km, together with values of $\langle\langle K_z\rangle\rangle$ for ozone, water vapour and aircraft-emitted $NO_x$, which apart from prescribed sources and sinks, were treated as tracers.

The right side of equation (2), the term $\overline{P^{\dagger}-L^{\dagger}}$, is the net source term. In practice it includes fluxes from the planetary surface, losses due to rainout and the like, but in the upper stratosphere may be dominated by terms from chemical kinetic rate equations.

If the aircraft-emitted $NO_x$ in the three-dimensional model is considered for the purpose of this exercise to be NO (there was no photochemistry in the model), the local value of the rate of the reaction

$$NO+O_3 \longrightarrow NO_2+O_2;\ k=9.5\times10^{-13}\exp(-1230/T)\,cm^3\,s^{-1}$$

may be computed, at any specified time, for each grid point. Averaging these local rates (which will be functions of the local values of [NO], [$O_3$] and $T$) over longitude will give zonal mean rates at any level. This true zonal mean rate,

$$\bar{P}_{\text{true}}=\overline{k[NO][O_3]}, \qquad (21)$$

may be compared with a zonal mean rate calculated by obtaining the product of the zonal means $\bar{k}$, $\overline{[NO]}$ and $\overline{[O_3]}$:

$$\bar{P}_{2D}=\bar{k}\,\overline{[NO]}\,\overline{[O_3]}. \qquad (22)$$

If there are significant differences between the values of $\bar{P}$ given by (21) and (22), then two-dimensional models are limited in accuracy to that extent in evaluating the rate of the reaction since they implicitly use (22).

A similar exercise was performed with two-dimensional model results, using (10*a*) and (10*b*), in order to examine the validity of one-dimensional evaluations of averaged rates. The three-dimensional model data were also further averaged down to true hemispheric mean and global mean values for the reaction between NO and $O_3$.

The reaction mechanism and rate coefficients used in the two-dimensional model are given in table 1.

The two-dimensional results used in this work have come from the Meteorological Office model described originally in Comesa (1975) and later updated and improved; see Murgatroyd (1977). It will suffice to say here that the model is formulated in 12 columns at 15° intervals from pole to pole and has 24 levels from surface to 48 km. The transport is in terms of $\bar{v}, \bar{\omega}(=\mathrm{d}p/\mathrm{d}t)$, where $p$ is pressure, and the eddy diffusion coefficient components $K_{yy}$, $K_{yz}$ and $K_{zz}$. The mean circulation data derive from climatological data up to about 30 km in the Northern Hemisphere, and up to 16 km in the Southern Hemisphere (see, for example, Newell *et al.* 1974) and from three-dimensional model calculations at higher levels. $\bar{\omega}$ was obtained from $\bar{v}$ by integrating the mass

continuity equation downwards from the top boundary, where $\bar{\omega} = 0$. The values for $K_{yy}$, $K_{yz}$ and $K_{zz}$ are based on those of Luther (1973) but somewhat larger values were used in the Northern Hemisphere winter, and smaller values in the Southern Hemisphere winter. The pattern of variance in $\bar{v}$ over a year's run from the Meteorological Office three-dimensional model (Comesa 1975; O'Neill & Newson 1977) was used as a guide for modifications to the $K$'s.

Table 1. Chemical kinetic mechanism, two-dimensional model

| | | $k$/(cm$^3$ molecule s units) |
|---|---|---|
| 1. | $O_2 + h\nu \longrightarrow O + O$ | photodissociation rates diurnally and seasonally time-dependent |
| 2. | $O_3 + h\nu \longrightarrow O_2 + O(^1D)$ | |
| 3. | $O_3 + h\nu \longrightarrow O + O_2$ | |
| 4. | $NO_2 + h\nu \longrightarrow NO + O$ | |
| 5. | $HNO_3 + h\nu \longrightarrow OH + NO_2$ | |
| 6. | $NO + h\nu \longrightarrow N + O$ | |
| 7. | $O(^1D) + M \longrightarrow O + M$ | $3.2 \times 10^{-11}$ |
| 8. | $O + O_2 + M \longrightarrow O_3 + M$ | $1.1 \times 10^{-34} \exp(507/T)$ |
| 9. | $O + O_3 \longrightarrow O_2 + O_2$ | $1.9 \times 10^{-11} \exp(-2300/T)$ |
| 10. | $NO + O_3 \longrightarrow NO_2 + O_2$ | $9.5 \times 10^{-13} \exp(-1230/T)$ |
| 11. | $NO_2 + O \longrightarrow NO + O_2$ | $9.1 \times 10^{-12}$ |
| 12.† | $O(^1D) + N_2O \longrightarrow NO + NO$ | $5.5 \times 10^{-11}$ |
| 13.‡ | $OH + NO_2 (+M) \longrightarrow HNO_3 (+M)$ | $k_{13}$ |
| 14. | $OH + O_3 \longrightarrow HO_2 + O_2$ | $1.6 \times 10^{-12} \exp(-1000/T)$ |
| 15. | $O(^1D) + H_2O \longrightarrow OH + OH$ | $1.75 \times 10^{-10}$ |
| 16. | $O + HO_2 \longrightarrow OH + O_2$ | $4.3 \times 10^{-11}$ |
| 17. | $N + NO \longrightarrow N_2 + O$ | $2.7 \times 10^{-11}$ |
| 18. | $N + O_2 \longrightarrow NO + O$ | $1.1 \times 10^{-14} T \exp(-3150/T)$ |
| 19. | $N + O_3 \longrightarrow NO + O_2$ | $5.7 \times 10^{-13}$ |
| 20. | $OH + HO_2 \longrightarrow H_2O + O_2$ | $2.0 \times 10^{-11}$ |

† Other channel to $N_2 + O_2$ allowed for at same rate.
‡ $k_{13} = k_a k_b[M]/(k_a + k_b[M])$; $k_a = (68 - 0.22T) \times 10^{-12}$; $k_b = 3.7 \times 10^{-32} \exp(1093/T)$.

The averaging of two-dimensional model dynamical representations to obtain one-dimensional dynamical parameters may be considered (Murgatroyd 1977). This can be done globally to obtain $\langle K_z \rangle$ as defined by (13), or hemispherically, as defined by (15).

Globally, by combining (9), (10$a$) and (13),

$$-\langle K_z \rangle \frac{\partial \langle \chi \rangle}{\partial z} = \frac{1}{2} \int_{-\frac{1}{2}\pi}^{\frac{1}{2}\pi} \left( \overline{w}\overline{\chi} - K_{yz} \frac{\partial \overline{\chi}}{\partial y} - K_{zz} \frac{\partial \overline{\chi}}{\partial z} \right) \cos\phi \, \mathrm{d}\phi = \left\{ \langle \overline{w}\overline{\chi} \rangle - \left\langle K_{yz} \frac{\partial \overline{\chi}}{\partial y} \right\rangle - \left\langle K_{zz} \frac{\partial \overline{\chi}}{\partial z} \right\rangle \right\}. \quad (23)$$

Then,

$$\langle K_z \rangle \frac{\partial \langle \chi \rangle}{\partial z} = A + \left\langle K_{zz} \frac{\partial \overline{\chi}}{\partial z} \right\rangle. \quad (24)$$

Since in (24) $A$ is dependent on $\overline{\chi}$ and its horizontal but not its vertical gradient, species with these parameters equal must have different values of $\langle K_z \rangle$, which may be negative.

By using (9), (10$b$) and (15) a similar relation may be deduced for the hemispheric case:

$$\langle\langle K_z \rangle\rangle \frac{\partial \langle\langle \chi \rangle\rangle}{\partial z} = \left\langle \left\langle K_{yz} \frac{\partial \overline{\chi}}{\partial y} \right\rangle \right\rangle + \left\langle \left\langle K_{zz} \frac{\partial \overline{\chi}}{\partial z} \right\rangle \right\rangle - \langle\langle w \rangle\rangle \langle\langle \chi \rangle\rangle - \langle\langle \overline{w}^* \overline{\chi}^* \rangle\rangle, \quad (25)$$

where $\overline{w} = \langle\langle w \rangle\rangle + \overline{w}^*$ and $\overline{\chi} = \langle\langle \chi \rangle\rangle + \overline{\chi}^*$.

From (25) it follows that even when the hemispheric mean vertical motion is resolved into mean and eddy components, species with the same values and horizontal gradients (which are in general small compared to vertical gradients) but different vertical gradients will have different

$\langle\langle K_z\rangle\rangle$ values. If the species further have vertical gradients of opposite sign, the $\langle\langle K_z\rangle\rangle$ values may be of opposite sign.

In summary, the numerical work done with the use of (1)–(25) and the Meteorological Office two-dimensional (Comesa 1975; Murgatroyd 1977) and three-dimensional (Comesa 1975; O'Neill & Newson 1977) models was as follows:

(i) Mean Northern Hemispheric values of $\langle\langle w\rangle\rangle$ and $\langle\langle K_z\rangle\rangle$ (for $O_3$, $H_2O$ and $NO_x$) were obtained by averaging three-dimensional model data at 6 h intervals over 30-day periods for a year (days 90–450 of the integration); the value for the first day of each month was also calculated.

(ii) The values of $\langle\langle w\rangle\rangle$ and $\langle\langle K_z\rangle\rangle$ for the first day of each month were similarly obtained for the Southern Hemisphere.

(iii) The zonal means $\bar{P}_{\text{true}}$ and $\bar{P}_{\text{2D}}$ defined by (21) and (22) were evaluated on days 180 and 360 (January and July solstices) of the three-dimensional integration.

(iv) The true column means $\langle k[\text{NO}]\,[\text{O}_3]\rangle$ and $\langle\langle k[\text{NO}]\,[\text{O}_3]\rangle\rangle$ in one dimension were also obtained on these days of the three-dimensional integration for the global, Northern and Southern Hemisphere cases, and compared with the one-dimensional model means $\langle k\rangle\langle[\text{NO}]\rangle\langle[\text{O}_3]\rangle$ and $\langle\langle k\rangle\rangle\langle\langle[\text{NO}]\rangle\rangle\langle\langle[\text{O}_3]\rangle\rangle$.

(v) The two-dimensional model data were averaged to produce one-dimensional data according to equations (23) and (25), for days 7380 (July solstice) and 7560 (January solstice) of an integration, at noon (the model included diurnal variations).

(vi) The same two-dimensional data were used to evaluate and compare the true global column mean $\langle\bar{k}[\overline{\text{A}}]\,[\overline{\text{B}}]\rangle$ of each of the rates of the reactions in table 1 with the one-dimensional model mean $\langle\bar{k}\rangle\langle[\overline{\text{A}}]\rangle\langle[\overline{\text{B}}]\rangle$. A similar calculation was done for the corresponding hemispheric means. It may be noted that the value of $\langle\langle K_z\rangle\rangle$ from the three-dimensional model was calculated as the hemispheric mean of negative values of the ratio of the local vertical eddy flux to the local vertical gradient of the appropriate tracer.

## 3. Results

A comparison of figures 1*a* and 1*b* shows the difference between monthly values obtained by averaging over 6 h intervals, and the values from a single day at the start of each month. The smoothing effect is not large; the data in figure 1*b* and *c* show that just 12 single-day values at monthly intervals draw up to a smooth contour diagram. Comparison of figures 1*b* and 1*c* shows that at any given time the Northern Hemisphere $\langle\langle w\rangle\rangle$ is closely balanced by a Southern Hemisphere $\langle\langle w\rangle\rangle$ of the same magnitude but opposite sign. A clear asymmetry between the hemispheres is revealed; the Northern Hemisphere summer has larger and more persistent positive $\langle\langle w\rangle\rangle$ values than the Southern Hemisphere summer, presumably because of the relatively greater extents of land in the Northern Hemisphere and of ocean in the Southern Hemisphere.

Figures 2*a* and 2*b* show the smoothing effect of the time averaging on $\langle\langle K_z\rangle\rangle$ ($O_3$) in the same way as did figure 1*a* and *b* for $\langle\langle w\rangle\rangle$. The differences are not large, and the general pattern in the Northern Hemisphere is of larger stratospheric values from November to April. Owing to the large computational burden, the Southern Hemisphere data have not been time-averaged, but if the same correspondence between the 12 single-day monthly values and the fully time-meaned values exists, figure 2*c* reveals a rather different structure for the mean hemispheric vertical eddy transport. Smaller values are widespread, and there is only a suggestion of the winter structure





PHILOSOPHICAL TRANSACTIONS OF THE ROYAL SOCIETY A MATHEMATICAL, PHYSICAL & ENGINEERING SCIENCES

seen in figure 2*b*. These systematic differences between the hemispheres and seasons were noted in previous work (Tuck 1977) where (13) was applied to the separate hemispheres.

The time-meaned pattern of $\langle\langle K_z \rangle\rangle$ values occurring for $NO_x$ and $H_2O$ in the Northern Hemisphere are broadly similar to that for $O_3$, as may be seen by comparing figures 2*a*, 3*a* and 3*b*, but with some differences near the tropopause and in the upper stratosphere.

The Southern Hemisphere spot values for $NO_x$ and $H_2O$ corresponding to figure 2*b* and 2*c* show similar large areas of small values, with negative areas constituting a substantial fraction of the total.

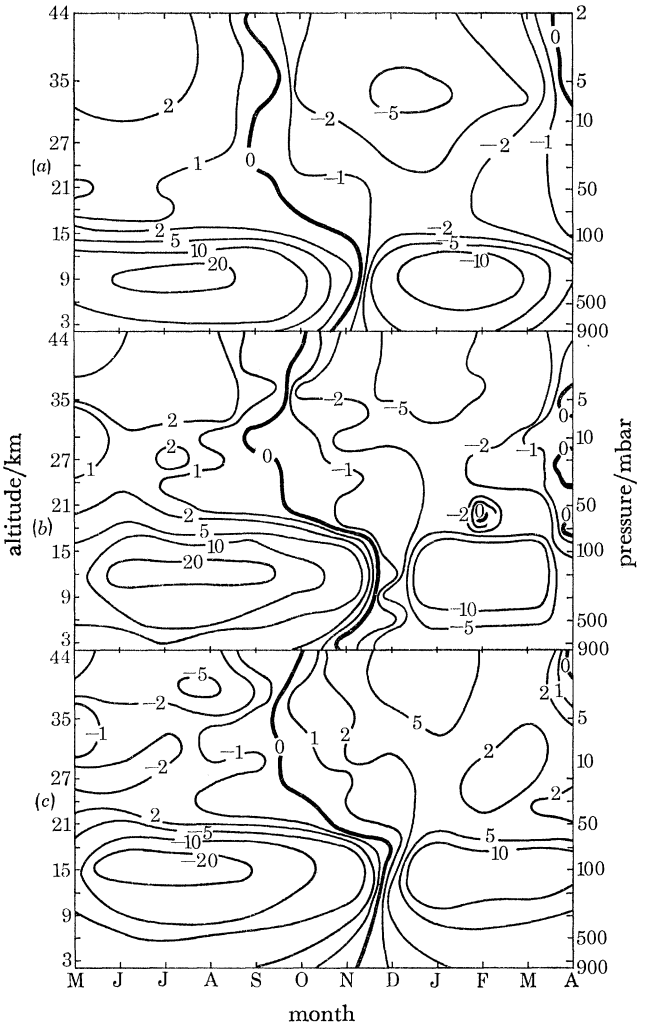


FIGURE 1. Mean hemispheric vertical velocities, three-dimensional model. Contours are $10^{-4}$ ms$^{-1}$. (*a*) N. Hemisphere, 30 day means from data at 6 h intervals; (*b*) N. Hemisphere, 30 day spot values; (*c*) S. Hemisphere, 30 day spot values.

A comparison of the hemispheric mean vertical velocities at winter and summer solstices reveals that in the troposphere the three-dimensional model values are considerably larger than the two-dimensional model values, as seen in figure 4. In the July stratospheres the values are quite similar, but in January the three-dimensionally derived values of $\langle\langle w \rangle\rangle$ are consistently larger than those obtained from the two-dimensional model data.

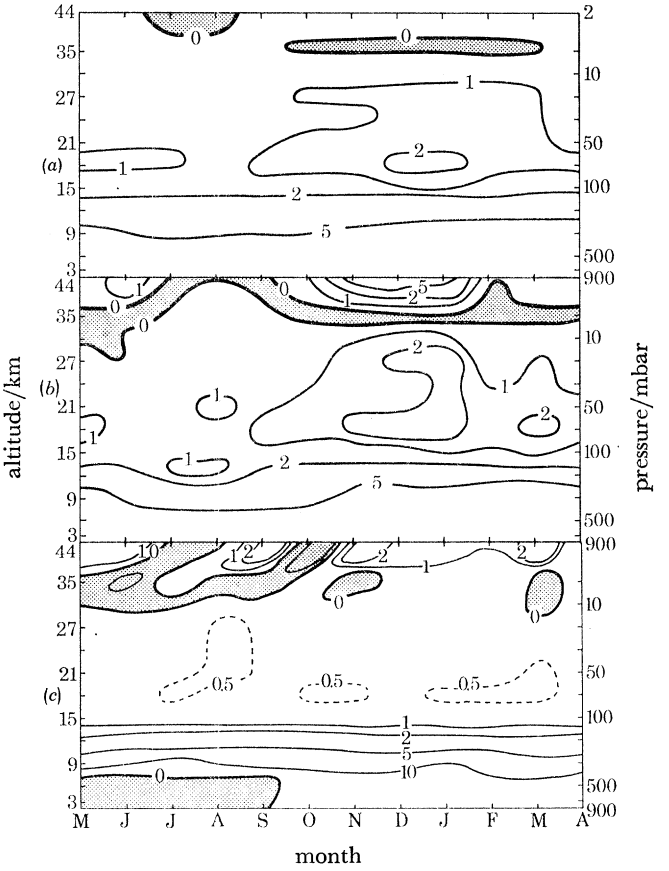


FIGURE 2. $\langle\langle K_z \rangle\rangle$ ($O_3$), three-dimensional model. Contours are $m^2\ s^{-1}$; shaded areas are negative. (*a*) N. Hemisphere, 30 day means from data at 6 h intervals; (*b*) N. Hemisphere, 30 day spot values; (*c*) S. Hemisphere, 30 day spot values.

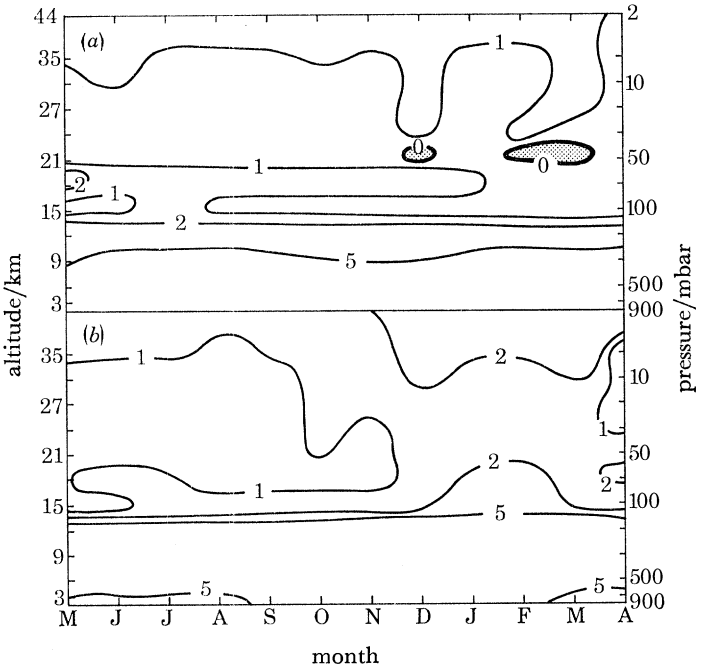


FIGURE 3. $\langle\langle K_z \rangle\rangle$ ($H_2O$) and $\langle\langle K_z \rangle\rangle$ ($NO_x$), three-dimensional model. Contours are $m^2\ s^{-1}$. (*a*) $\langle\langle K_z \rangle\rangle$ ($H_2O$), 30 day means from data at 6 h intervals; (*b*) $\langle\langle K_z \rangle\rangle$ ($NO_x$), 30 day means from data at 6 h intervals.

Space does not permit extensive display of three-dimensional and two-dimensional model results used as inputs in this work; descriptions may be found in Comesa (1975), Murgatroyd (1977) and in O'Neill & Newson (1977). However, much of the work on average rates of chemical reactions was done with two-dimensional model latitude–height cross sections, and as an indicator of the model's ability to produce a reasonable ozone cross section, figure 5 is included.

The computation of global values of $\langle K_z \rangle$ from averaging of the two-dimensional model dynamical parameters is shown in figure 6 only for nitrous oxide (exemplifying a species well mixed in the troposphere, and mixing ratio decreasing with height in the stratosphere) and for total odd nitrogen (exemplifying a species with a stratospheric mixing ratio maximum and a

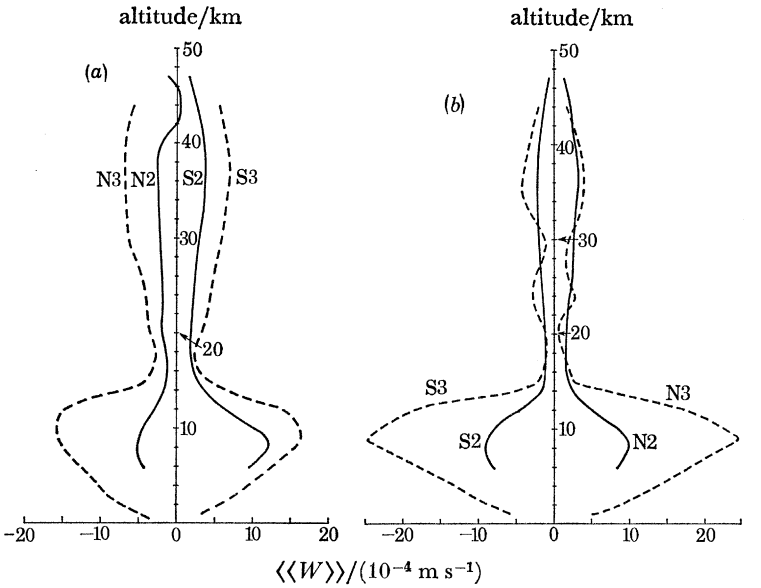


Figure 4. Mean hemispheric vertical velocities, two-dimensional and three-dimensional models. (*a*) January solstice; (*b*) July solstice. N2, N. Hemisphere, two-dimensional; S2, S. Hemisphere, two-dimensional; N3, N. Hemisphere, three-dimensional; S3, S. Hemisphere, three-dimensional.

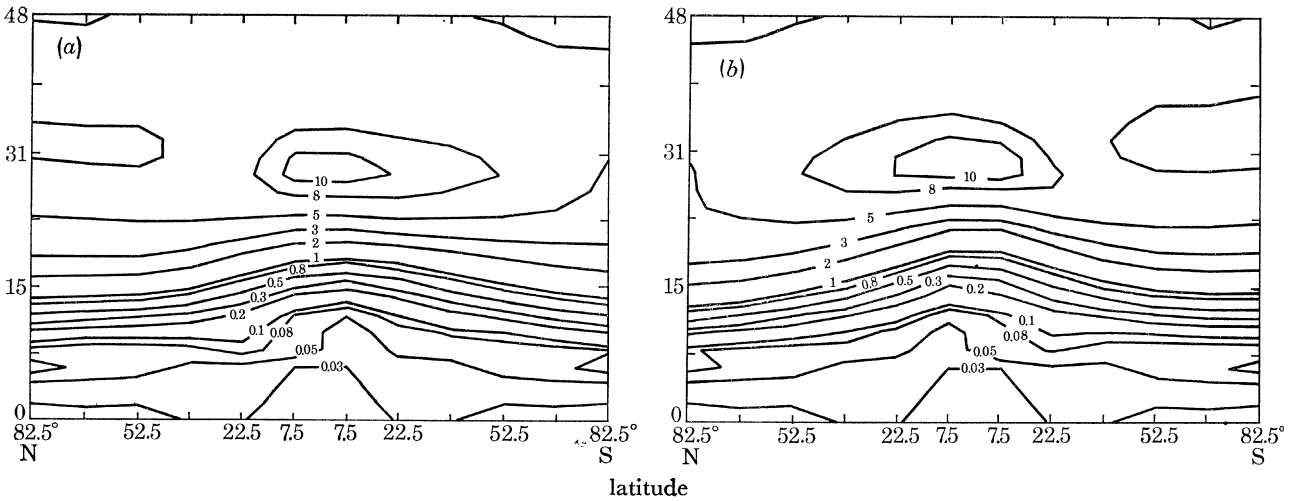


Figure 5. Two-dimensional model $(Z, \phi)$ ozone cross sections. (*a*) $O_3$ volume mixing ratio contours, solstice, year 21; (*b*) $O_3$ volume mixing ratio contours, July solstice, year 20.

downwards directed gradient above the tropopause). The profiles are different for the two types of tracer, and $\langle K_z \rangle$ is not well behaved near the tropopause for $N_2O$, or near the photochemical source region for $(NO + NO_2 + HNO_3)$. Similar results were obtained for $H_2O$ (like $N_2O$) and $O_3$ (like odd nitrogen, but more variable). An attempt to obtain hemispheric mean values for a total flux-based $\langle\langle K_z \rangle\rangle$ from (13) produced profiles with large negative excursions and generally erratic behaviour.

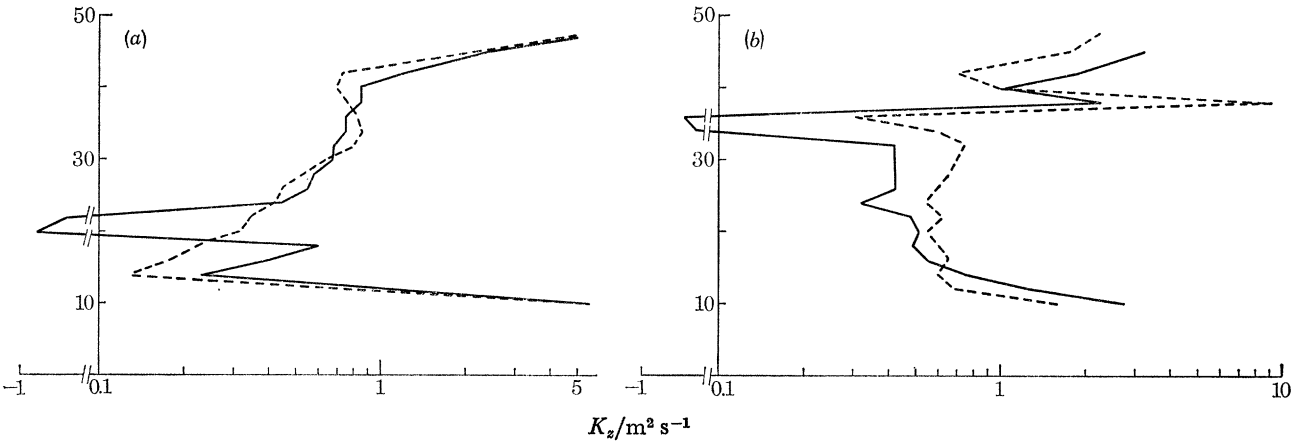


FIGURE 6. $K_z$ profiles from averaging two-dimensional model data. (*a*) $\langle K_z \rangle$ ($N_2O$), January and July solstices; (*b*) $\langle K_z \rangle$ ($NO + NO_2 + HNO_3$), January and July solstices. Solid line, January; broken line, July.

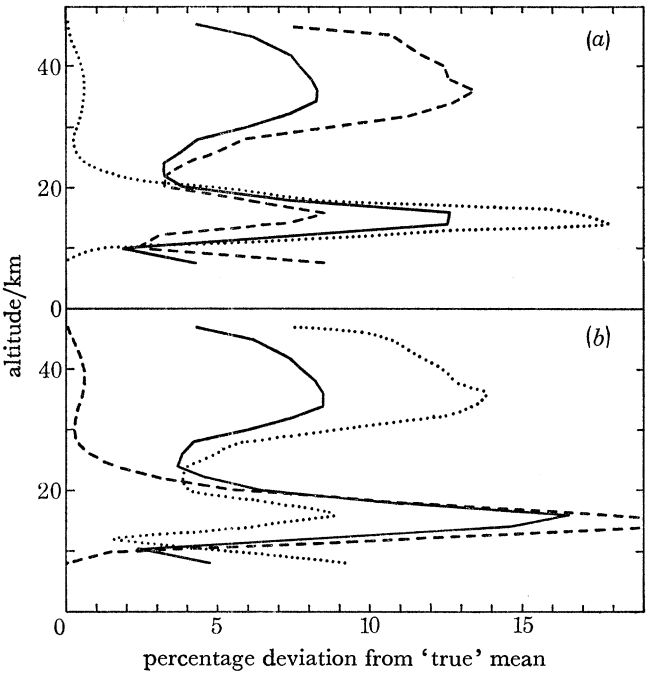


FIGURE 7. Averaging two-dimensional model rates to one dimension;

$k[O]\,[O_2]\,[M]$, the rate of $O + O_2 + M \longrightarrow O_3 + M$.

(*a*) January solstice, year 21; (*b*) July solstice, year 20. Solid line, global mean; broken line, N. Hemisphere mean; dotted line, S. Hemisphere mean.

Although the averaging of two-dimensional model fields of molecular number densities, rate coefficients and reaction rates was carried out for all the reactions in table 1 (except photodissociations), the results are illustrated here only for reactions 8, 11 and 13; figures 7, 8 and 9 respectively show the percentage deviation of the one-dimensional model mean $\langle\bar{k}\rangle\langle[\overline{A}]\rangle\langle[\overline{B}]\rangle$ from the 'true' global mean $\langle\bar{k}[\overline{A}]\,[\overline{B}]\rangle$. A consistent pattern is clear: there are at both times, in global and hemispheric cases, significant deviations in the upper troposphere and lower stratosphere. In the winter hemisphere, there are significant deviations in the middle and upper stratospheres. In the summer hemisphere, this region shows reasonable agreement between the means. The lower values in figure 7 occur because O atoms are better correlated with $O_3$ molecules than for example, with $NO_2$. The deviations in figure 8 are caused almost entirely by the covariance of OH and $NO_2$ rather than by the pressure and temperature dependence of the reaction rate.

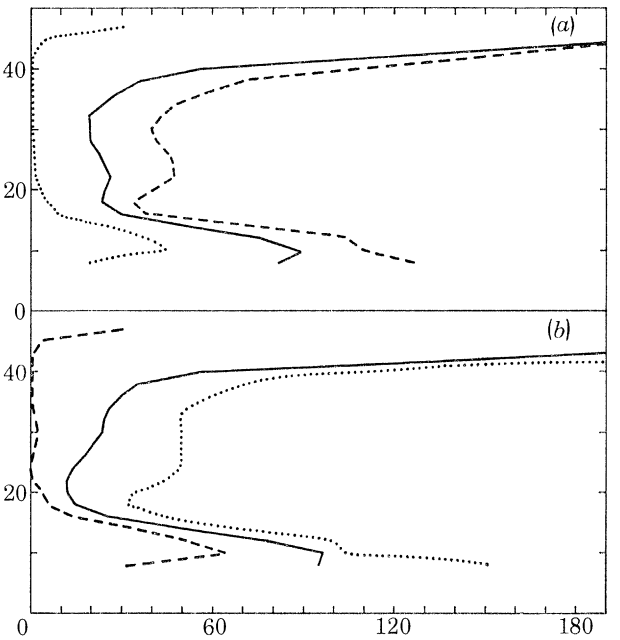


FIGURE 8.

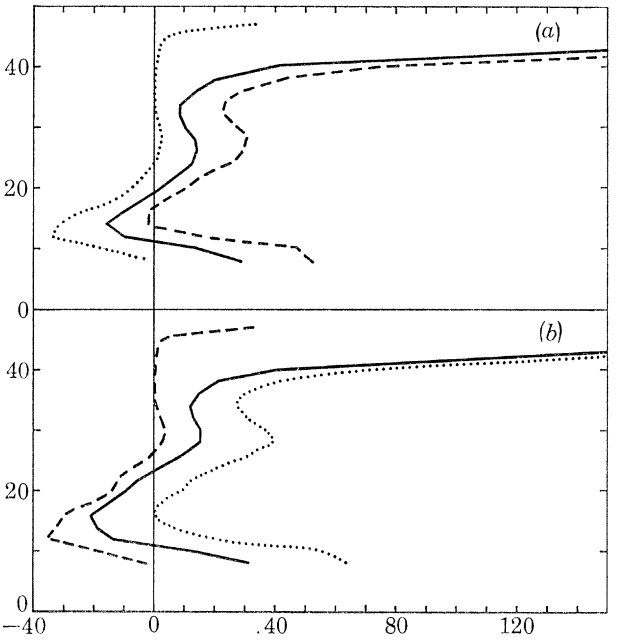


FIGURE 9.

FIGURE 8. Averaging two-dimensional model rates to one dimension; $k[OH]\,[NO_2]$ (see table 1), the rate of $OH+NO_2(+M)\longrightarrow HNO_3(+M)$. (*a*) January solstice, year 21; (*b*) July solstice, year 20. Solid line, global mean; broken line, N. Hemisphere mean; dotted line, S. Hemisphere mean.

FIGURE 9. Averaging two-dimensional model rates to one dimension; $k[NO_2][O]$, the rate of $NO_2+O\longrightarrow NO+O_2$. (*a*) January solstice, year 21; (*b*) July solstice, year 20. Solid line, global mean; broken line, N. Hemisphere mean; dotted line, S. Hemisphere mean.

The deviation is most serious for reaction 13, and is mainly caused by nonlinear correlations between OH and $NO_2$, rather than by pressure or temperature dependence. The nature of the effect is for the one-dimensional model mean to overestimate the rate of reactions 8 and 13; for reaction 11 the tendency is to overestimate in the winter hemisphere, to be quite accurate in the summer stratosphere, and to underestimate in the summer tropopause region.

The quantity $100\,(\bar{P}_{\text{true}}-\bar{P}_{\text{2D}})/\bar{P}_{\text{true}}$, the percentage difference between the true and two-dimensional model means, was evaluated at January solstice (360 days) and July solstice (180 days) of the three-dimensional model integration. The resulting data are plotted respectively in




PHILOSOPHICAL TRANSACTIONS OF THE ROYAL SOCIETY A MATHEMATICAL, PHYSICAL & ENGINEERING SCIENCES

figures 10*a* and 10*b*, and clearly display the regions of inadequacy of two-dimensional models in calculating the rate of reaction of aircraft injected $NO_x$ with $O_3$. In agreement with the two-dimensional model averaged to one dimension, the only region of accuracy is the middle stratosphere in summer. It is of interest that in January the three major regions of negative anomaly in the zonal mean reaction rate are associated with a westerly jet; the region of positive anomaly is in the broad location of the source of aircraft emission of $NO_x$. Virtually all the deviation in $\bar{P}_{2D}$ arises from nonlinear correlation between NO and $O_3$, with only a small component from the products $k[NO]$ and $k[O_3]$. The July zonal means of the reaction rate again show large negative anomalies associated with the tropospheric jets; there is, however, no area of negatives associated with the Southern Hemisphere polar night vortex. A very intense area of large positive anomalies (up to 80 %) occurs near the surface in mid-latitudes, particularly in the Northern Hemisphere. The covariance $\overline{[H_2O]'[O_3]'}$ caused a different effect; the quantity $100(\bar{P}_{true}-\bar{P}_{2D})/\bar{P}_{true}$ had large positive values up to 90 % around tropospheric westerly jets, and negative values as low as $-20$ % above the equatorial tropopause.

TABLE 2. THREE-DIMENSIONAL DATA AVERAGED TO ONE DIMENSION

$\langle k\rangle\langle[NO]\rangle\langle[O_3]\rangle/\langle k[NO]\,[O_3]\rangle$ and $\langle\langle k\rangle\rangle\langle\langle[NO]\rangle\rangle\langle\langle[O_3]\rangle\rangle/\langle\langle k[NO]\,[O_3]\rangle\rangle$.

Single angle brackets represent a global average, and double angle brackets a hemisphere average.

| global Jan. | N. Hem. Jan. | S. Hem. Jan. | global July | N. Hem. July | S. Hem. July | Pressure mbar† |
|---|---|---|---|---|---|---|
| 0.985 | 0.891 | 1.039 | 0.822 | 0.993 | 0.685 | 2 |
| 1.057 | 0.912 | 1.135 | 0.762 | 1.022 | 0.647 | 5 |
| 1.122 | 1.024 | 1.191 | 0.869 | 1.036 | 0.774 | 10 |
| 1.311 | 1.232 | 1.440 | 1.041 | 1.106 | 1.064 | 20 |
| 1.264 | 1.181 | 1.426 | 1.066 | 1.089 | 1.230 | 30 |
| 1.235 | 1.187 | 1.461 | 1.091 | 1.088 | 1.601 | 50 |
| 0.825 | 0.795 | 1.273 | 0.687 | 0.710 | 1.528 | 70 |
| 0.508 | 0.533 | 1.053 | 0.471 | 0.497 | 1.378 | 100 |
| 0.397 | 0.524 | 1.116 | 0.456 | 0.458 | 1.418 | 200 |
| 0.566 | 0.659 | 1.379 | 0.687 | 0.583 | 1.404 | 300 |
| 0.885 | 0.912 | 1.392 | 1.205 | 0.881 | 1.516 | 500 |
| 0.938 | 0.966 | 1.459 | 1.315 | 0.936 | 1.430 | 700 |
| 0.992 | 1.016 | 1.466 | 1.942 | 1.147 | 1.439 | 900 |

† 1 mbar = $10^2$ Pa.

Figure 10*a* and 10*b* demonstrate that two-dimensional models will not be able to model tropospheric chemistry in a quantitative manner; problems also occur in the lower stratosphere, particularly in winter.

The last results are shown in table 2, and consist of the three-dimensional data for $k[NO]\,[O_3]$ averaged down to one dimension. The data clearly show hemispheric asymmetries, with $\pm 50$ % deviations from the true mean occurring. The meridional variance has in some cases, particularly in the Southern Hemisphere, outweighed the zonal variance causing the anomalies in figure 10*a* and 10*b*. The data of table 2 may be compared with figures 7–9, which display the equivalent one-dimensional results from averaging the two-dimensional model.





PHILOSOPHICAL TRANSACTIONS OF THE ROYAL SOCIETY A MATHEMATICAL, PHYSICAL & ENGINEERING SCIENCES

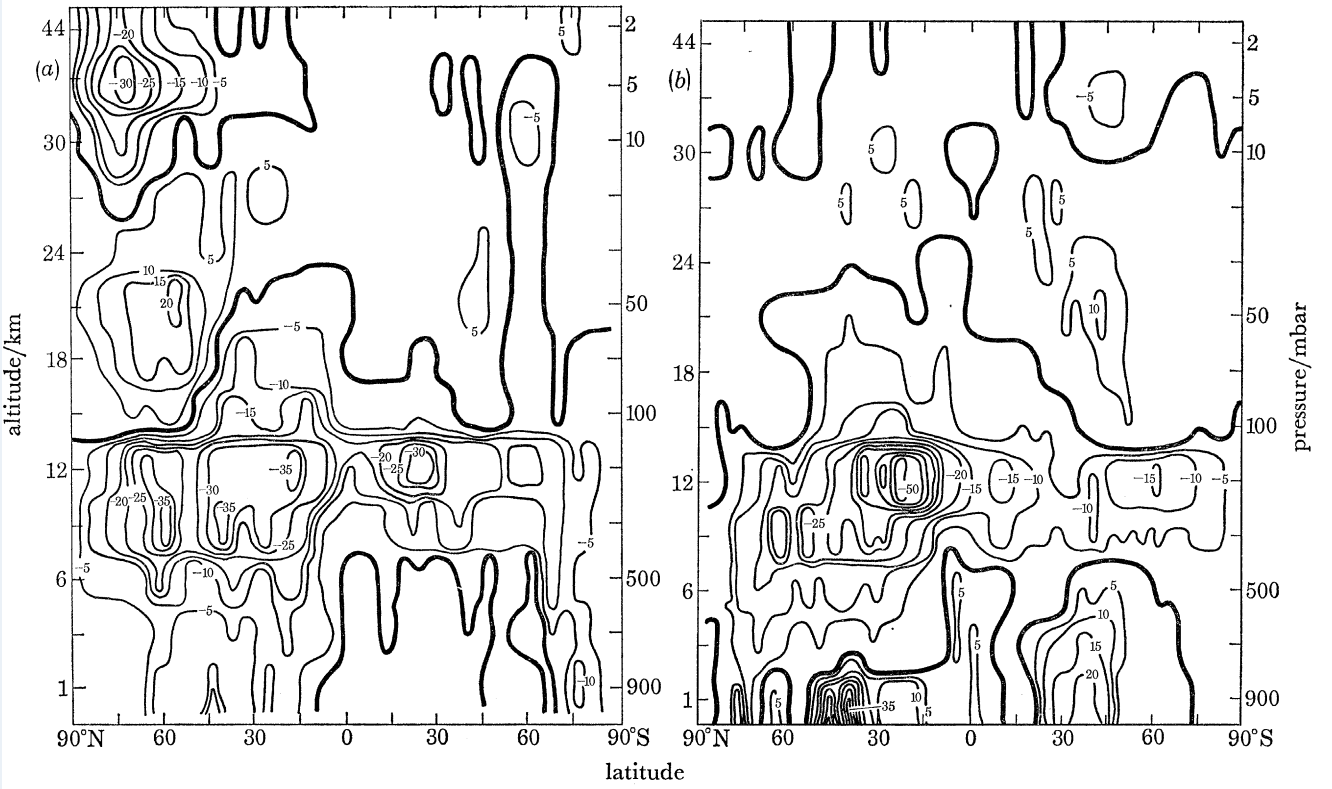


FIGURE 10. Averaging three-dimensional model rates to two dimensions;

$$k[\mathrm{NO}]\,[\mathrm{O_3}], \quad \text{the rate of} \quad \mathrm{NO} + \mathrm{O_3} \longrightarrow \mathrm{NO_2} + \mathrm{O_2}.$$

Contours are percentage deviation of $\overline{k}\;\overline{[\mathrm{NO}]}\;\overline{[\mathrm{O_3}]}$ from $\overline{k\,[\mathrm{NO}]\,[\mathrm{O_3}]}$. [NO] is effectively a gaseous tracer for aircraft emissions in the three-dimensional model. (*a*) January solstice, day 360; (*b*) July solstice, day 180.

## 4. Discussion and conclusions

Before considering in detail the results obtained in § 3, it is essential to realize that the ideal way of computing the zonal, hemispheric or global mean of a particular quantity is by using local measurements distributed throughout the real atmosphere. Should the very large volume of data needed for this task ever be acquired, it would then be possible to check experimentally the averaging assumptions incorporated in models of varying dimensionality. Meanwhile, it can be said that as regards chemical composition, the real atmosphere is likely to be inhomogeneous and to have nonlinear correlations between species on a much larger range of scales than is encompassed by the models used here. This is particularly true of the smaller scales, which tend to be missing or badly represented in the models. The estimates of the deviations of zonal, hemispheric and global mean rates of reactions from their 'true' values obtained in this work are therefore likely to be lower than is really the case in the atmosphere. To this extent, they therefore represent an optimistic picture of the ability of current models to compute mean rates of chemical reactions in the atmosphere, and perturbations caused by gases emitted as a result of human activities.

Considering now the specific results described in § 3, it is clear that as far as the three-dimensional model is concerned, there is a distinct asymmetry between the hemispheres in the atmospheric dynamics when these are averaged down to a single column (representing a

hemispheric mean). The upward vertical velocities occurring in the Northern Hemisphere summer troposphere have larger magnitudes than those occurring in the Southern Hemisphere summer troposphere. It is apparent from figure 1 that mean upward velocities in the Northern Hemisphere model troposphere (balanced by downward velocities in the Southern Hemisphere troposphere) persist for about $7\frac{1}{2}$ months from May to November inclusive; there are thus approximately $4\frac{1}{2}$ months in the Northern Hemisphere with mean tropospheric vertical velocities direct downwards. In the stratosphere, the position is different. The larger values tend to occur in the Southern Hemisphere summer, and persist in an upwards direction for 6–7 months from October to April, with corresponding negative values in the Northern Hemisphere winter. The results must be viewed with caution, since the Southern Hemisphere simulation in the troposphere is not as good as the Northern Hemisphere simulation (Comesa 1975). The subtropical jet was too far north, and tropospheric eddy activity (cyclones and anticyclones) was concentrated not at about 60 °S, but was also too far north. The three-dimensional model integration of 450 days contained two northern winters but only one southern one, and it is possible that a second southern hemisphere winter might have been an improvement. However, both Northern Hemisphere winters included periods where sudden warming events occurred, whereas none occurred in the Southern Hemisphere. Both Northern and Southern Hemisphere stratospheres were reasonable simulations, with some shortcomings such as too strong a polar night vortex.

It is perhaps worth stressing that the fundamental hemispheric asymmetry in the model derives from the distribution of land and oceans, and the consequent differences in surface temperature and exchanges. In the real atmosphere, effects such as aircraft operations and chlorofluoromethane releases are heavily biased towards the Northern Hemisphere; thus, subject to the admitted imperfections of the three-dimensional model, it may be concluded that hemispheric asymmetries should be taken into account in perturbation calculations. This is highlighted by the fact that values of the hemispheric mean vertical velocity, $\langle\langle w\rangle\rangle$, are heavily influenced (because of $\cos\phi$ weighting) by the upward branch of the Hadley Cell occurring in tropical regions, and the upward extension of this motion is in turn the largest component in the air inflow to a hemispheric stratosphere (Reiter 1975). Manabe & Mahlman (1976) have also noted substantial asymmetries between hemispheres in a general circulation model integration.

The Northern Hemisphere pattern of higher values of up to $2\,m^2\,s^{-1}$ during winter (when there was a sudden warming) and values from 0.2 to $1.0\,m^2\,s^{-1}$ in summer shows a clear seasonal variation in the eddy transfer, for all three tracers. The rather different vertical eddy transfer coefficients, $K_z$, derived for the Southern Hemisphere are of interest. It has been noted previously (Tuck 1977) that there is no *a priori* reason to expect $K$-theory to apply to vertical transfer in the atmosphere, and hence negative values are not excluded in principle and in fact occur.

The vertical eddy transfer is then seasonally dependent in the Northern Hemisphere, as are the vertical motions. Thus, on a hemispheric basis, faster chemistry in the summer is correlated with mean upward motion and slower vertical eddy transfer. The reverse situation pertains in winter with slower photochemistry, mean downward motion and faster eddy transfer. No one-dimensional model to date has accommodated these correlations.

The eddy transfer coefficients, $K_z$, from the three-dimensional model show a sensitivity to the location of the tracer sources and sinks. Mahlman (1976) has reached a similar conclusion. The values of $K_z$ derived from averaging the two-dimensional model data and dynamical parameters show clear disruption near the tropopause for nitrous oxide, and immediately above the ozone layer maximum for odd nitrogen. The profiles are different for different tracers, and different at





PHILOSOPHICAL TRANSACTIONS OF THE ROYAL SOCIETY A MATHEMATICAL, PHYSICAL & ENGINEERING SCIENCES

summer and winter solstices for the same tracer. These conclusions are again serious for one-dimensional modelling, since models to date have used a single, time-invariant $K_z$ profile.

The results of averaging two-dimensional model fields to obtain hemispherically and globally averaged rates of reaction showed systematic deviations from the 'true' global mean $\overline{k[\mathrm{A}]\,[\mathrm{B}]}$ by the one-dimensional model global mean $\bar{k}\,\overline{[\mathrm{A}]}\,\overline{[\mathrm{B}]}$. These deviations were larger in the winter hemisphere, and generally showed a maximum near the tropopause. Within the model limitation, it may be concluded from figures 7–9 that a one-dimensional model only computes the rate of a gas reaction accurately in the middle and upper stratosphere in summer. This is when the photochemistry is dominant, and it may be concluded that at other times and in other places the two-dimensional model dynamics are giving rise to nonlinear correlations between species which cause serious deviations in the one-dimensional average rate.

The conceptual errors occurring here in the estimation of the rates of individual gas kinetic processes will, in a model calculation, combine to produce a cumulative effect. The magnitude of the error so induced in any particular photochemical calculation could only be assessed accurately for a one-dimensional model by running it in models of two and three dimensions. Inspection of figures 7–10 and table 2 suggests that it could be quite large.

The association of the maximum negative anomalies in the zonal mean rate $\bar{k}\,\overline{[\mathrm{NO}]}\,\overline{[\mathrm{O_3}]}$ (calculated from the three-dimensional model), with westerly jet streams in figure 10*a*, strongly suggests that the nonlinear correlations between $[\mathrm{NO}_x]$ and $[\mathrm{O_3}]$ are caused by large-scale eddy fluxes, which also tend to be highly correlated with jet maxima. The consequences for atmospheric chemistry are considerable. For example, the rate of any reaction in the upper troposphere or winter stratosphere cannot be reliably computed in even a two-dimensional model; the concept of a single mean tropospheric lifetime for a species reacting in a temperature-dependent manner with a tropospheric mean value of [OH], for example, is seriously undermined. Nonlinear correlations near corridors of aircraft operation in the lower stratosphere render two-dimensional model calculations inaccurate in computing the rate at which aircraft-emitted nitrogen oxides will react with ozone. The further averaging to one dimension makes one-dimensional averages worse still, with the meridional variance sometimes opposing the zonal variance, and at other times reinforcing it.

It seems likely that while eddy vertical transfer may be significant (but not dominant) in the three-dimensional model Northern Hemisphere, vertical transfer of materials in the Southern Hemisphere is achieved to a greater extent by the mean motion; other significant asymmetries involve the extent and persistence of seasonal variations in mean hemispheric vertical velocities.

The deviations occurring from 'true' mean rates of reaction in the course of averaging both three- and two-dimensional models suggest a consistent picture of maximum anomalies occurring in regions where dynamical features tend to be prominent: for example near jet streams, the tropopause region and in the winter stratosphere.

A factor which may explain the large errors in zonal means near tropospheric jet streams is the structure of tropospheric depressions in mid and high latitudes. These phenomena are regarded as eddies on the global scale, but on a scale of *ca.* $10^3$ km possess distinct organization, with a warm sector from low latitudes separated from colder high latitude air by frontal systems, in which rainout of soluble species may occur (the three-dimensional model $\mathrm{NO}_x$ had a rainout sink). Tropopause folding and stratosphere–troposphere interchanges are known to be associated with depressions, fronts and jet streams; since warm sector air probably has a different chemical composition from cold sector air, nonlinear correlations may occur in these localities. The





PHILOSOPHICAL TRANSACTIONS OF THE ROYAL SOCIETY A MATHEMATICAL, PHYSICAL & ENGINEERING SCIENCES

deviations near the polar night jet in the Northern Hemisphere may occur because the sudden warming similarly exchanges large volumes of air of different origins (and therefore different chemical compositions). The errors near the Southern Hemisphere polar night vortex are much smaller, possibly because no sudden warming event occurred.

It should be realized that the real atmosphere is likely to be more inhomogeneous than even the three-dimensional model. For example, according to Riehl & Malkus (1958) the upward branch of the Hadley circulation may be accounted for globally by the operation of a few thousand cumulonimbus cores in the tropics. These events, occurring on a scale too small for explicit representation in a three-dimensional g.c.m., thus collectively form the dynamical feature which is the major source of air for the stratosphere (Reiter 1975). It may be true that they are sources of nitric oxide, produced by lightning discharges (Tuck 1976); they are certainly a sink for soluble tropospheric gases by means of rainout processes, see, for example, Junge (1963). There are thus likely to be significant departures from homogeneity as regards chemical composition in these events which are significant globally but too localized for specific formulation in a g.c.m.

Burnett (1976) has recorded observations of OH column densities fluctuating by factors between 5 and 10 during daylight hours, from day to day. Such observations are difficult to explain in any way other than by highly nonlinear correlations between the number densities of different gases. It follows that it is of great interest to obtain simultaneous measurement of molecular concentrations in both time and space; simultaneous observations of $NO_2$, $O_3$ and OH column densities from the ground are currently feasible, for example.

Since the checking of model calculations of rates of reaction by measurements is likely to be limited for some time to come, it may be worth examining an alternative modelling approach. It should be possible to compute Lagrangian air trajectories from meteorological observations, and perform model chemical calculations as a function of latitude, longitude, pressure and temperature along the path of the air parcel chosen, including if necessary some representation of the effect of any cloud or precipitation processes observed. Comparison of different trajectories would then yield information about correlations between species.

The final observation which may be made as a result of this examination of model assumptions and data is that one and two-dimensional models of the sort widely used for perturbation calculations of the effect of aircraft and chlorofluoromethanes on the stratospheric ozone balance (C.I.A.P. 1974; Booker 1975; Comesa 1975; N.R.C. 1976) are unreliable tools for quantitative estimation of rates of gas reactions in the atmosphere. This is because nonlinear correlations, arising largely from dynamical phenomena, are either ignored or inadequately represented. The resultant errors come from the design of one- and two-dimensional models rather than from the input data, and so have not been included in published estimations of error limits associated with ozone perturbation calculations.

The author wishes to express his appreciation to R. J. Murgatroyd for many valuable discussions and suggestions. Thanks are also due to M. K. Hinds and S. A. Clough for two-dimensional model data in advance of publication. D. W. Jones, K. S. Groves and D. Jerrett all helped with the computation at various times.





PHILOSOPHICAL TRANSACTIONS OF THE ROYAL SOCIETY A MATHEMATICAL, PHYSICAL & ENGINEERING SCIENCES

## References (Tuck)

Burnett, C. R. 1976 *Geophys. Res. Lett.* **3**, 319–322.
Booker, H. G. 1975 *Environmental impact of stratospheric flight.* Washington, DC: Climatic Impact Committee, National Academy of Sciences.
C.I.A.P. 1974 *Climatic Impact Assessment Program. Report of findings.* Cambridge, Mass.: U.S. Department of Transportation.
Comesa 1975 *The report of the Committee on Meteorological Effects of Stratospheric Aircraft 1972–1975.* Bracknell: U.K. Meteorological Office.
Gudiksen, P. H., Fairhall, A. W. & Reed, R. J. 1968 *J. geophys. Res.* **73**, 4461–4473.
Junge, C. E. 1963 *Air chemistry and radioactivity.* New York: Academic Press.
Luther, F. M. 1973 *A.I.A.A./A.M.S. Int. Conf., Denver, Colorado*, A.I.A.A. paper 73–498.
Mahlman, J. D. 1976 *Proc. 4th Conf. on C.I.A.P.*, DOT-TSC-OST-75-38. Cambridge, Mass.: U.S. Department of Transportation.
Manabe, S. & Mahlman, J. D. 1976 *J. Atmos. Sci.* **33**, 2185–2217.
Murgatroyd, R. J. 1977 *Proc. Scient. Seminar on Stratospheric Monitoring.* Paris Sécretariat d'Etat Auprès du Ministre de l'Equipement (Transports).
N.R.C. 1976 *Halocarbons: effects on stratospheric ozone.* Washington, D.C.: National Academy of Sciences.
Newell, R. E., Kidson, J. W., Vincent, D. G. & Boer, G. J. 1974 *The general circulation of the tropical atmosphere*, vols 1 and 2. Cambridge, Mass.: M.I.T. Press.
O'Neill, A. & Newson, R. L. 1977 *IAMAP, Comm. Met. Upper Atmos., Coll. Ext. Summ.*, Seattle, pp. 50-1–50-6.
Reed, R. J. & German, K. E. 1965 *Mon. Weath. Rev.* **93**, 313–321.
Reiter, E. R. 1975 *Rev. Geophys. Space Phys.* **13**, 459–474.
Riehl, H. & Malkus, J. S. 1958 *Geophysica* **6**, 505–538.
Tuck, A. F. 1976 *Q. Jl R. met. Soc.* **102**, 749–756.
Tuck, A. F. 1977 *Proc. R. Soc. Lond.* A **355**, 267–299.

### *Discussion*

R. A. Scriven (*Central Electricity Research Laboratories, Kelvin Avenue, Leatherhead, Surrey*). Dr Tuck has demonstrated very clearly that some care is required in constructing global averages and interpreting the results from sample models. Does this not mean that the measurement of a few variables at a few points on the Earth cannot be taken to describe events over the Earth as a whole? Is the information on $CO_2$, for example, sufficient for us to be able to say with certainty that the total amount of $CO_2$ in the Earth's atmosphere is increasing at 0.25 % per annum? Perhaps Dr Tuck's models can be used to tell us what the existing measurements really do mean and what further measurements are required.

A. F. Tuck. The covariance of reactants will mean that it may be difficult to estimate a global budget for reactive species with short lifetimes using measurements at a few locations. For species with longer lifetimes, the effectiveness will depend on the patchiness of the distribution of its sources and sinks. In the case of $CO_2$, it is my impression that a small number of stations would give a reliable estimation of global amounts.

D. T. Swift-Hook (*Central Electricity Research Laboratories, Kelvin Avenue, Leatherhead, Surrey*). Dr Tuck's diagrams showed that vertical variations of the different quantities in time and place are apparently striated in about half a dozen steps. Have these layers any physical reality or are they simply artefacts of the computing, due perhaps to a coarse mesh?

A. F. Tuck. It must be remembered that the three-dimensional model has 13 levels up to 44 km; the vertical resolution of about 3 km is rather coarse for really good reproduction of features like jet streams and the tropopause.